Asian Journal of Chemistry; Vol. 36, No. 10 (2024), 2253-2259

ASIAN JOURNAL OF CHEMISTRY

https://doi.org/10.14233/ajchem.2024.31954

Enhanced Catalytic Activity for Production of Biodiesel from *Aloe vera* Oil and the Removal of Methyl Violet Dye using Polyaniline-Fe_3O_4 Magnetic Nanocomposite

NARENDRA MAHADU PATIL[1], ANNAPURNA JHA[2], VISHNU A. ADOLE[3], NANASAHEB P. HUSE[4] and MANOHAR R. PATIL[1,*]

[1]Department of Chemistry, Nandurbar Taluka Vidhayak Samiti's, G.T. Patil Arts, Commerce and Science College, Nandurbar-425412, India
[2]Department of Chemistry, Jamshedpur Women's University, Jamshedpur-831004, India
[3]Department of Chemistry, MGV's Loknete Vyankatrao Hiray Arts, Science and Commerce College, Panchavati, Nashik-422003, India
[4]Advanced Nanomaterials and Interfaces Laboratory, Department of Physics, Nandurbar Taluka Vidhayak Samiti's G.T. Patil Arts, Commerce and Science College, Nandurbar-425412, India

*Corresponding author: E-mail: profmanoharpatil@gmail.com

Received: 15 May 2024; *Accepted*: 16 July 2024; *Published online*: 30 September 2024; AJC-21754

The aim of this work was to use a unique technique to maximize the efficiency and cost-effectiveness of biodiesel synthesis utilizing *Aloe vera* oil. Moreover, in order to facilitate the magnetic separation from the resultant mixture, lipase was immobilized on a magnetic nanocomposite consisting of polyaniline (PANI) and Fe_3O_4. Utilizing XRD, SEM, TGA and FTIR spectroscopy, the nanocomposite was thoroughly characterized. The results indicated that the immobilized lipase exhibited enhanced thermal stability and a modified optimum pH compared to its free form. Using immobilized lipase also significantly improved the biodiesel conversion yield from 27% with free enzyme to 60%. Remarkably, after five cycles of reutilization in the production of biodiesel, the immobilized lipase retained 90% activity. The catalytic effectiveness of lipase during biodiesel synthesis was significantly enhanced and its resistance to heat and pH fluctuations was strengthened by this novel immobilization approach. Beyond its potential usage in biodiesel production, the PANI-Fe_3O_4 magnetic nanocomposite also demonstrated photocatalytic removal and degradation of methyl violet dye from aqueous solution.

Keywords: PANI–Fe_3O_4 magnetic nanocomposites, Lipase, Immobilization, Biodiesel, Methyl violet dye.

INTRODUCTION

Biodiesel is a renewable fuel derived from organic materials like plants and animals. It shares qualities with traditional diesel, making it suitable for use in existing diesel engines [1,2]. In response to the environmental worries and dwindling reserves of critical resources such as crude oil and coal, biodiesel has emerged as an alternative to petroleum-based diesel. The demand for energy worldwide continues to surge, projected to spike by 56% between 2010 and 2040 as reported by Energy Information Administration (US EIA, 2013) [3]. The escalating population growth and the shift toward better living standards coupled with increased urbanization have notably contributed to this challenge. Consequently, there is a concerted push to tackle environmental concerns, notably the exhaustion and escalating prices of fossil fuels like natural gas, petroleum and coal, through extensive research into alternative energy sources, particularly renewable energy.

Biodiesel, comprised of long-chain fatty acid methyl esters (FAME), has garnered worldwide interest as a readily deployable replacement for traditional fossil fuels in this context [4]. As a renewable energy source, biodiesel made from vegetable oil has a lot of potential. For producing biodiesel, numerous procedures using biochemical or enzyme catalysis or a supercritical CO_2 environment have been devised [5-7]. The ongoing burning of fossil fuels has resulted in the release of dangerous gases such particulate matter, CO, SOx and NOx. It puts human life at risk for several major health problems [8,9]. The quantity of various wastes generated has increased in tandem with the world population's rapid growth. As a result, there is a pressing need for efficient waste disposal methods [10,11]. Since enzyme the transesterification of lipids is a sustainable method of producing renewable fuels, it is a good substitute for chemical procedures. Because of its selectivity and low temperatures, enzymatic catalysis produces highly pure products while still being environmentally benign.

Edible and non-edible oils are used to create biodiesel in numerous nations. However, the high cost of vegetable oil means that biodiesel is 1.5 times more expensive than fossil fuel, which restricts its widespread use [12]. For this reason, waste oil was chosen as the study's feedstock to produce biodiesel. Numerous studies have been published on the enzymatic catalysis of freed or immobilized lipases in the generation of biodiesel. Researchers have become interested in enzymatic transesterification with lipase to produce biodiesel in recent years. The lipase enzyme (EC 3.1.1.3, triacylglycerol hydrolases) can be used to produce biodiesel because of its outstanding catalytic activity even in non-aqueous conditions. When it comes to biodiesel manufacturing, lipase outperforms chemical catalysis in several ways. These include minimum wastewater treatment requirements, fast glycerol recovery and no adverse effects [13,14]. Because immobilized lipases are easily retrieved from the reaction mixture, they are helpful for the continuous generation of biodiesel. Numerous techniques for immobilizing lipase have been documented, including as entrapment, covalent immobilization, adsorption as well as whole cell biocatalysts [15,16].

The adsorption and covalent immobilization techniques are the least expensive and most successful immobilization techniques available. One of the simplest techniques is adsorption, although this type of biocatalyst typically lacks the degree of stability that is obtained by covalent binding since the binding of enzymes to matrices is frequently poor. When compared to alternative techniques, covalent immobilization yields the strongest enzyme support link. Lipases need to be strong and flexible at the same time because a flexible active site can withstand stress without becoming less active. Strong multipoint covalent bonds, however, increase the possibility of irreversible active site deformation and function loss. To increase the immobilization effectiveness and stability of *A. niger* (RM1265) lipase, we employed an intermediate technique in this study that falls among adsorption and covalent bonding. Nanoparticles preserved in lipases serve as efficient catalysts for biodiesel production [17].

Immobilization using magnetic nanocomposites has been used for magnetic lipase methods since they are cost-effective and the total surface area of reaction mixture is enhanced by small particle size. Thus, in this study, to methanize waste oil, *Aspergillus niger* lipase (RM1265) was first immobilized on an active PANI-Fe_3O_4 magnetic nanocomposite. Additionally, the PANI-Fe_3O_4 magnetic nanocomposite is shown to be an effective catalyst for methyl violet dye degradation.

EXPERIMENTAL

Aspergillus niger lipase (RM1265) was supplied by HiMedia Laboratories Pvt. Ltd., India, whereas *p*-nitrophenol palmitate was procured from Sigma-Aldrich, USA. The other reagents and solvents used were of AR grade and purchased from different reputed commercial suppliers. The Soxhlet extractor was used to extract oil from dried *Aloe vera* leaves.

Modification of nanocomposite: Lipase was immobilized using a polyaniline (PANI)–Fe_3O_4 magnetic nanocomposite, which was prepared *in situ* by self-polymerizing aniline monomer [18]. The magnetic nanocomposite exhibited a transformation after 5 g were refluxed in 25 mL of ethanolamine. The nanocomposite was air dried and rinsed three times with 60 mL of acetone following a 3 h reflux. After that, 25 mL of 4% (w/v) glutaraldehyde in 50 mM phosphate buffer (pH 8) was added to activate the magnetic nanocomposite and the mixture was stirred gently at 40 ºC for 2 h. The active magnetic nanocomposite was washed with phosphate buffer to remove glutaraldehyde.

Immobilization of lipase: After mixing 25 mL of lipases with 0.1 mL of Tween 80 in 50 mM phosphate buffer (pH 8) and stirring for 5 min, 5 g of PANI-Fe_3O4 magnetic nanocomposite was added. After the addition of 100 mL of cold acetone, the mixture was agitated for 0.5 h at 40 ºC. Filtered lipase immobilized by magnetic nanocomposite was lyophilized after being rinsed with 25 mL of cold acetone.

Lipase assay: *p*-Nitrophenol palmitate was used as substrate in a spectrophotometric lipase assay [19]. The amount of lipase that releases 1 µmol of *p*-nitrophenol per min under assay conditions is known as one unit (U) of lipase.

Characterization: The XRD spectra were recorded with a Bruker D8 Advance X-ray diffractometer using Cu*K*α1 radiation X-ray source having a 1.5406 Å wavelength. The SEM analysis of modified nanocomposite and lipase immobilized modified nanocomposite were carried out using HITACHI-S-4800 (type II) instrument, Japan. Thermal analysis of modified nanocomposite and lipase immobilized modified nanocomposite were carried out using Thermal analyzer Perkin-Elmer Pyris-1 TGA. The FTIR analysis of modified nanocomposite and lipase immobilized modified nanocomposite were carried out on FTIR spectrometer Perkin-Elmer spectrum GX in the range of 4000 cm^{-1} to 370 cm^{-1}.

Effect of temperature and thermostability: The effect of temperature on the free and immobilized lipase activity was determined for *p*-nitrophenyl phosphate (*p*-NPP) hydrolysis. The hydrolysis of *p*-NPP was observed at various temperatures (20-70 ºC), where the *p*-NPP solution was pre-incubated to reach the desired temperature before the addition of lipase.

pH stability and thermostability: Following pre-incubating enzyme specimens at 300 ºC for 60 min at pH 4–11 [50 mM sodium acetate buffer (pH 5), 50 mM potassium phosphate buffer (pH 6), 50 mM Tris–HCl buffer (pH 8) and 50 mM glycine–NaOH buffer (pH 9)] [20,21]. The impact of pH on the free or immobilized enzymes was investigated. After that, remaining activity was measured using the industry standard procedures. Thermostability of the free and immobilized lipase activity was assessed by measuring the remaining enzyme activity at 37 ºC after 60 min of incubation in a phosphate buffer (50 mM, pH 7) at temperature ranging from 30 ºC to 90 ºC. The lipase that was not incubated was assumed to have 100% enzyme activity.

Biodiesel synthesis

Transesterification reaction: The transesterification reaction used to synthesize biodiesel was conducted at 50 ºC in screw-capped vials that were housed inside a reciprocating shaker. Aloe vera leaves were dried and oil was extracted from

the dried leaves by using Soxhlet extraction method. The oil extracted from Aloe vera was used as a raw material for biodiesel synthesis. The initial reaction mixture included the appropriate controls (samples devoid of enzyme), immobilized lipase 50 U, a butanol:oil volume ratio of 0.2 and an oil:methanol molar ratio of 1:2.

Sampling: Synthesis of fatty acid methyl ester was analyzed by modified hydroxamic acid method [22].

Operational stability of nanocomposite bound lipase: The functional reliability of isolated lipases was observed as well for the biodiesel synthesis. The immobilized lipases were collected when the reaction completed, and the reactants adsorbed on the matrix were eliminated by centrifuging them for 10 min at 5,000 rpm and washed them in hexane. After that, a fresh run of the immobilized lipases was initiated using the same reaction mixture composition and the biodiesel synthesis was assessed in the supernatant.

RESULTS AND DISCUSSION

Synthesis of biodiesel

Immobilization of enzyme: The process of immobilizing lipase was done on a modified crosslinked nanocomposite. The specific activity of the individual lipases before and after binding to the nanocomposite was used to assess the lipase immobilization yield. An immobilization efficiency of 85% was obtained on a modified crosslinked magnetic nanocomposite for lipase. Covalent immobilization of recombinant *Rhizopus oryzae* lipase onto three Purolite® supports treated with glutaraldehyde yielded a higher yield than earlier results [14,15]. The most effective technique for immobilizing enzymes is covalent attachment; nevertheless, due to the robust interactions that exist between the support and the enzyme, enzyme distortions can occasionally arise, resulting in denaturation and decreased enzyme activity. In current immobilization procedure, ethanolamine was first adsorbed on a nanocomposite, treated with glutaraldehyde and then immobilized using enzyme. As a result, lipase is effectively immobilized on activated nanocomposite without losing its enzyme function because this procedure is not entirely covalent attachment. It was found that the lipase's thermostability and immobilization yield are improved by the activated nanocomposite.

XRD studies: The XRD spectrum of the modified nanocomposite is shown in Fig. 1 and the results are summarized in Table-1. The obtained sharp and intense peaks confirm the prepared sample is of good crystallinity and is in good agreement with the JCPDS data (PDF# 01-078-6086) which confirms the formation of PANI-Fe_3O_4. Using Scherer's formula, which is displayed in eqn. 1, the average crystallite size was calculated from the XRD data and was around ~45.41 nm. The crystallite size (D) ranges from 22.05 nm to 94.25 nm, suggesting a variation in particle sizes within the sample. Dislocation density provides information about the amount of defects in the crystal lattice and microstrain indicates the strain within the crystal structure. Using the eqns. 2 and 3, the strain and dislocation density of the PANI-Fe_3O_4 were determined from the XRD data and given in Table-1.

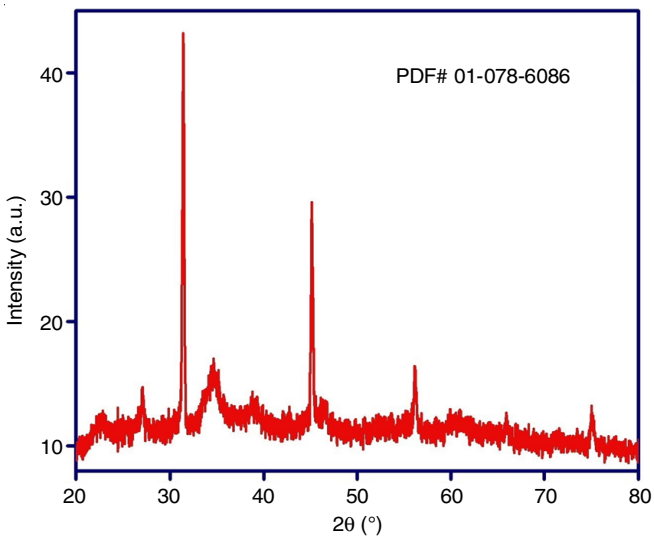

Fig. 1. XRD pattern of Fe_3O_4 magnetic nanocomposite

TABLE-1
STRUCTURAL PARAMETERS OBTAINED FROM XRD OF PANI/Fe_3O_4 NANOCOMPOSITE

2θ (°)	β (Rad)	D (nm)	δ (10^{14})	ε
27.00	0.004219286	33.70	8.75	0.001025653
31.39	0.003283238	43.80	5.19	0.000790181
34.65	0.015409778	94.25	1.13	0.003677523
45.13	0.003695302	40.60	6.05	0.000853046
56.14	0.004121683	38.10	6.87	0.000909120
75.00	0.007926460	22.05	20.50	0.001571803

$$D\ (khl) = \frac{0.9\lambda}{\beta\cos\theta} \quad (1)$$

$$\varepsilon = \frac{\beta\cos\theta}{4} \quad (2)$$

$$\delta = \frac{1}{D^2} \quad (3)$$

where D stands for crystallite size, λ represents wavelength of X-ray used (1.5406 Å), β stands for full width at half maximum (FWHM) of the peak, θ is the Bragg's angle, ε represents the strain and δ is the dislocation density.

SEM studies: Fig. 2a,c show the SEM images of the polyaniline/Fe_3O_4 magnetic nanocomposite confirmed the heterogeneous nautre and on the dark greyish polyaniline, there is a whitish cluster of Fe_3O_4 nanoparticles. Following activation with ethanolamine and glutaraldehyde, the lipase immobilized modified magnetic nanocomposites of polyaniline/Fe_3O_4, the surface displayed the high surface porosity and roughness (Fig. 2a,d).

Thermal studies: Thermal studies revealed that both the modified polyaniline and the enzyme-immobilized polyaniline are tolerant of thermal degradation as shown in Fig. 3a-b. The initial weight loss at 200 ºC was primarily caused by low molecular weight molecules and water evaporation. The doping agent degradation was linked to the second weight loss, which occurred between 220 and 300 ºC. The breakdown of polyaniline was linked to the weight loss at 400-500 ºC. Fe_3O_4 broke down from

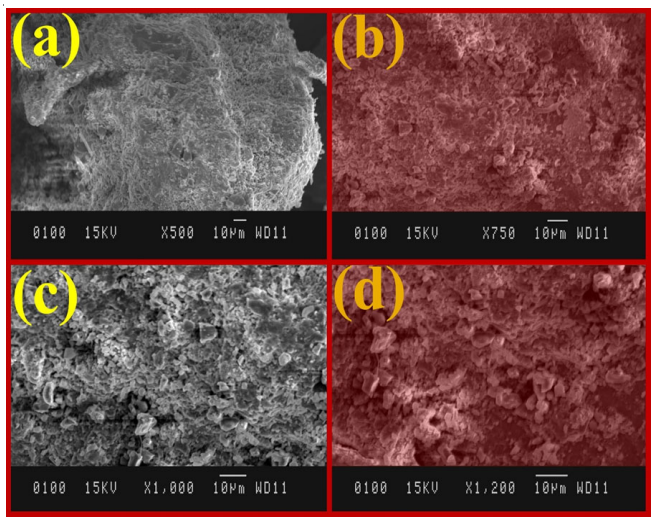

Fig. 2. SEM of lipase immobilized modified magnetic nanocomposites of polyaniline/Fe_3O_4 at various resolutions

covalently bound polyaniline at temperatures above 500 ºC. Fig. 3a (polyaniline-Fe_3O_4) and 3b (polyaniline-Fe_3O_4 enzyme nanocomposite) both showed this tendency. Nevertheless, Fig. 3b illustrates a slight increase in weight loss, which might be attributed to the incorporation of enzyme in the nanocomposite.

FT-IR studies: Fig. 4a-b display the FT-IR spectra of the enzyme-immobilized PANI-Fe_3O_4 nanocomposite and the activated PANI-Fe_3O_4 nanocomposite, respectively. The absorption band at 468 cm^{-1} is due of the stretching vibration of Fe–O. The N–H stretching and C–N stretching vibrations can be attributed to the peaks at 3408 cm^{-1}, 1112 cm^{-1} and 1070 cm^{-1}, respectively. The C=C stretching vibration of aromatic ring of aniline is responsible for the appearance at 1633 and 1620 cm^{-1}. Most of the peaks in Fig. 4a-b are similar, except for one peak at 2854 cm^{-1}, which might be related to the C-H stretching vibration of aldehydic group. This is because the free aldehyde group in activated PANI-Fe_3O_4 nanocomposite is used to immobilize lipase in enzyme-immobilized PANI-Fe_3O_4 nanocomposite.

Effect of temperature on lipase activity: Application of lipases in the chemical synthesis, especially biodiesel production, often leads to thermal inactivation due to denaturation of protein. Fig. 5 illustrates the effect of temperatures on free as well as enzyme-immobilized PANI-Fe_3O_4 nanocomposite. Up to 40 ºC, it was found that the activity of the immobilized and free lipases was about equal, but at higher temperatures, the immobilized lipases was more stable and exhibited a modest increase in the activity. This hypothesis is feasible due to the immobilization of enzymes by multiple point binding, resulting in an enhanced rigidity that is typically associated with improved resistance to thermal denaturation. In contrast to this, a study conducted by Kumar *et al.* [23] showed that activity of purified lipase increased by ~50% in the presence of all the tested commercial detergents at a temperature ranging from 5 to 60 ºC.

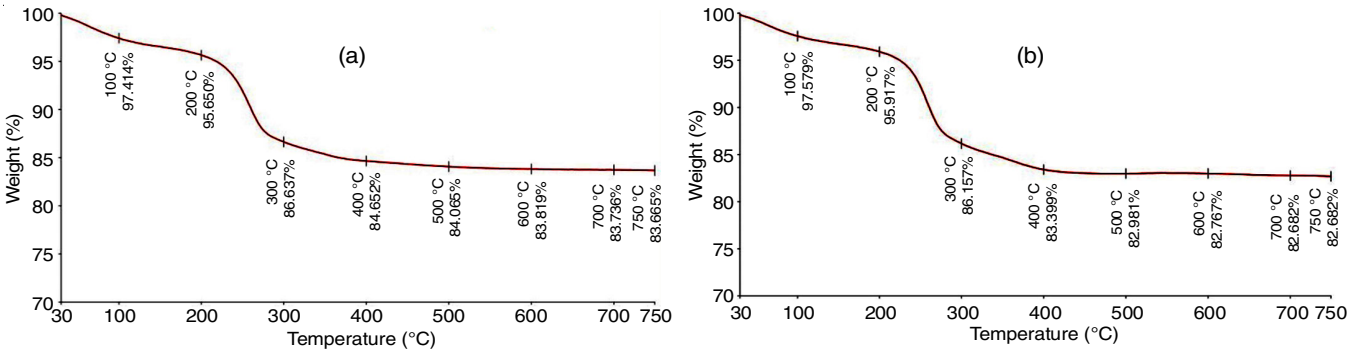

Fig. 3. Thermograms of PANI-Fe_3O_4 magnetic nanocomposite modified after treatment with ethanolamine and glutaraldehyde (a) and lipase immobilized modified magnetic nanocomposite (b)

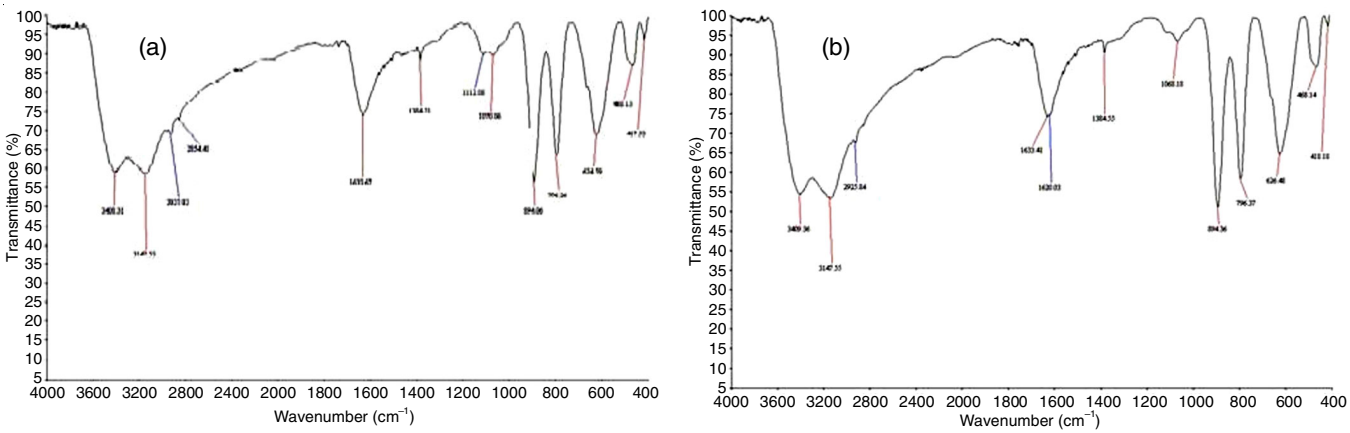

Fig. 4. FTIR spectra of PANI-Fe_3O_4 magnetic nanocomposite modified after treatment with ethanolamine and glutaraldehyde (a) and lipase immobilized modified magnetic nanocomposite (b)

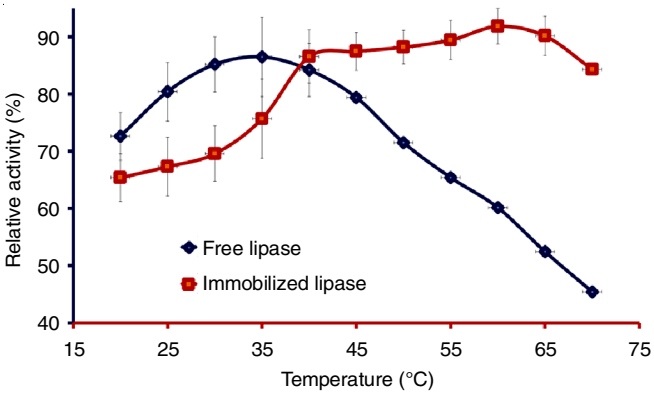

Fig. 5. Effect of temperature on free and immobilized lipase. Data are represented as the mean ± standard deviation of three replications

Thermostability of free and immobilized lipases: The present investigation examined the thermal stability of both soluble and immobilized lipase across a range of temperatures, spanning from 300 to 900 ºC (Fig. 6). It was shown that immobilized lipase intacted all its activity, whereas free lipase activity declined at 400 ºC and remained inactive after 600 ºC. It has been observed that the immobilized lipase maintained 84% of its initial activity after 1 h of incubation, even at 900 ºC, while the free lipase stopped functioning well before this temperature. Several studies [24,25] have demonstrated that immobilized lipase is more stable than free lipase, but the thermal stability seen in this work was significantly better.

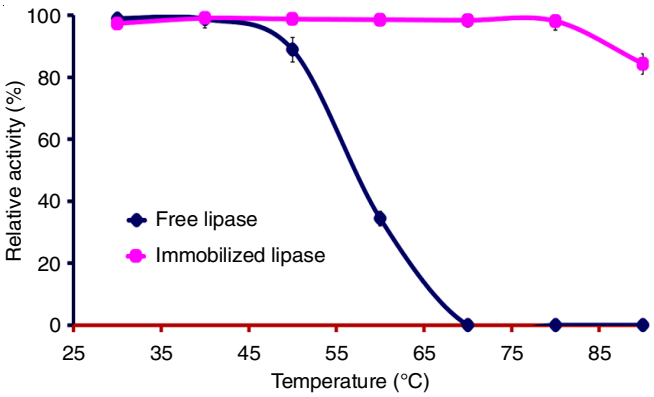

Fig. 6. Thermostability of free and immobilized lipase. Data are represented as the mean ± standard deviation of three replications

Effect of pH on lipase activity: Enzyme immobilization may be caused by the conformational changes in enzyme that alter ideal pH. The current finding indicates that both immobilized and free lipases remained stable throughout the pH range of 4 to 7. Immobilized lipase continued to function at pH 8 and below, whereas free lipase began to deactivate (Fig. 7). Due to the association between the enzyme and the activated magnetic nanocomposite, the denaturation of the enzyme at basic pH is prevented, resulting in enhanced stability of the immobilized lipase [26]. In contrast to this lipase with activity in a pH range of 7.6-8.6 with an optimum at 8 [27], pH range 8.0-10.5 with an optimum at 8.5 [28] and pH range 7-9 with an optimum at 8.5 [29] have been defined as alkaline in previous studies.

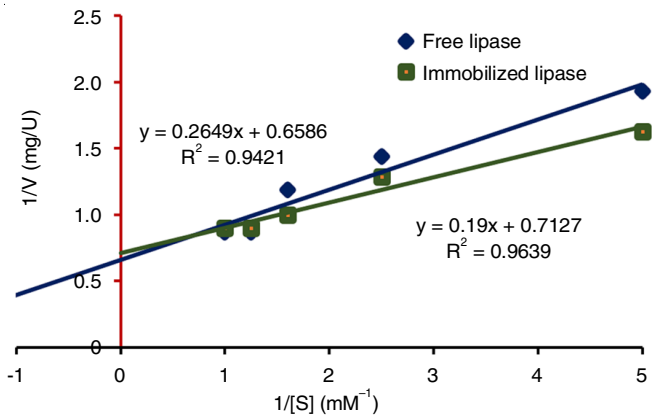

Fig. 7. Effect of pH on free and immobilized lipase. Data are represented as the mean ± standard deviation of three replications

Kinetic parameters of free and immobilized lipases: Derivation of the kinetic constants V_{max} and K_m from the double reciprocal plots shown in Fig. 8. Whereas immobilized lipase exhibited a K_m value of 0.27 mM and a V_{max} of 1.4 U/mg, free lipase displayed K_m values of 0.4 mM and V_{max} of 1.5 U/mg. The decrease in K_m value suggested that immobilization had enhanced the enzyme's affinity for the substrate [30,31]. The V_{max} values generally decrease during immobilization, which is consistent with other comparable findings [15].

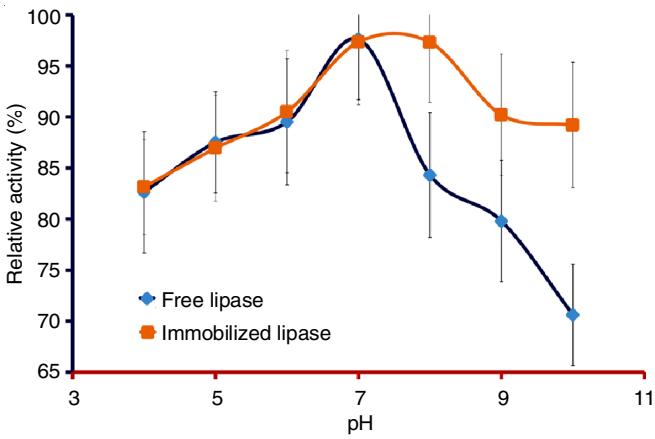

Fig. 8. Lineweaver-Burk plots for free and immobilized lipase

Synthesis of biodiesel by free and immobilized lipases: Studies on the solvent-free biodiesel synthesis capabilities of both free and immobilized lipases was carried out (Fig. 9). According to results, after 50 h of reaction time, immobilized lipase produced a greater percentage conversion of 60%; however, employing free lipase, the resultant conversion percentage does not surpass 27%. It was found that this finding outperformed earlier published ones [32]. The complex interaction between the enzyme and the activated nanocomposite, which prevents the enzymes from being distorted in the reaction mixture, could be the reason for the enhanced effectiveness of immobilized lipase in the production of biodiesel.

Operational stability of immobilized lipases: The stability of the immobilized lipase, which is a potential enzyme for industrial use, is a crucial factor that impacts the cost-effectiveness of the process. Fig. 10 illustrates that immobilized lipase can

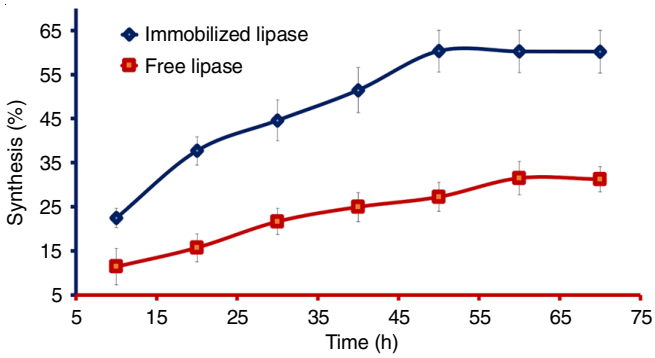

Fig. 9. Biodiesel synthesis with free and immobilized lipase. The results are represented as the mean ± standard deviation of three replications

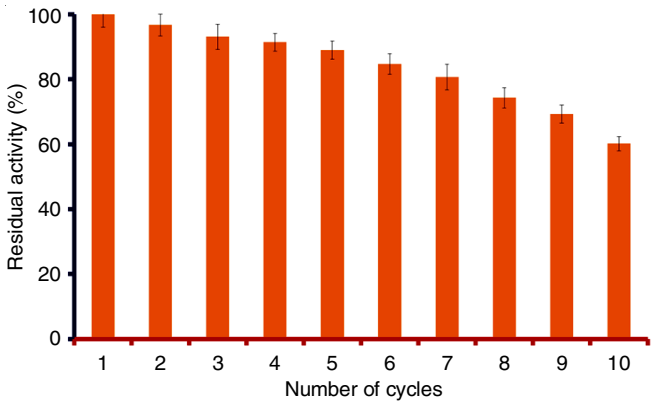

Fig. 10. Operational stability of immobilized lipases for biodiesel synthesis. Data are represented as mean ± standard deviation of three replications

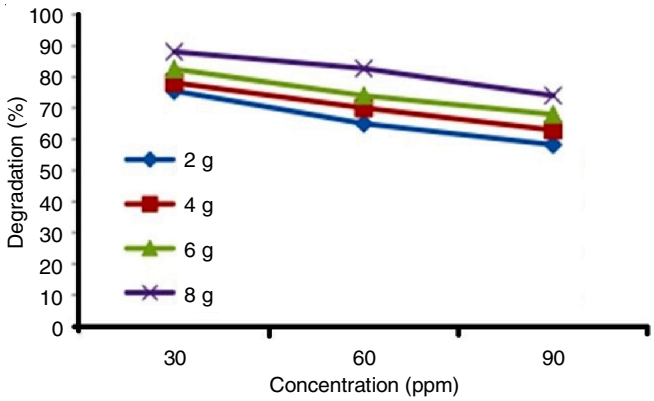

Fig. 11. Effect of photocatalyst dose on the removal of methyl violet dye at different initial dye conc. with contact time 120 min and pH 8.5

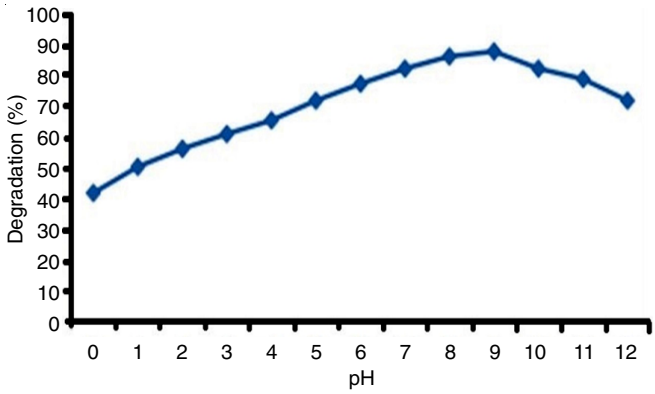

Fig. 12. Effect of pH on degradation of methyl violet dye by Fe_3O_4 catalyst having dosage 8 g/L at 30 ppm

be reused for up to five cycles while retaining over 90% of its initial activity when compared with the previous studies conducted by the researchers showed 84% activity up to 5 cycles and >66% activity after 10 cycles [33-35]. The good operational stability may be attributed to the close interaction between the matrix and the enzyme. The formation of Schiff's base between the side-chain amino groups of enzyme: and the free aldehyde groups of glutaraldehyde-treated nanocomposite is another explanation for the strong contact. Due to its remarkable stability, the enzyme immobilized on nanocomposite in organic solvent ensured good reusability for biodiesel synthesis.

Removal of methyl violet dye

Effect of catalyst dose: Using different doses of magnetic nanocomposite ranging from 2 to 8 g/L, the impact of catalytic dose on the degradation of methyl violet was examined. When the quantity of magnetic nanocomposite rises, photocatalytic destruction of methyl violet increases rapidly. Fig. 11 shows that as the number of active sites on catalyst increases, methyl violet dye degradation also increases.

Effect of pH: The breakdown of methyl violet dye through photocatalysis was investigated at varying pH levels, as it is a crucial factor in the surface reactions. At 30 ppm methyl violet dye and a magnetic nanocomposite concentration of 8 g/L, the function of pH in photocatalytic dye degradation was investigated in the pH range of 0-12. It was observed that the rate of photocatalytic degradation enhanced with an increase in pH up to 8.5 (Fig. 12). The number of anions increases as pH rises and a bond was formed between these anions and magnetic nanoparticles. As the pH increases beyond 8.5, the negatively charged surface of the magnetic nanoparticles repels the anions of methyl violet dye, reducing the efficacy of the dye's breakdown.

Conclusion

The work effectively reported that lipase can be immobilized on a PANI–Fe_3O_4 magnetic nanocomposite. Enhancing the enzyme's resistance to thermal denaturation and significantly increasing its efficacy in biodiesel production compared to its free state. Additionally, the PANI-Fe_3O_4 magnetic nanocomposite was also investigated as a photocatalyst, demonstrating remarkable performance in the breakdown of methyl violet dye. The intriguing immobilization method demonstrated excellent operational stability in the biodiesel synthesis while also speeding the chemical reactions at higher temperatures, indicating a great potential for organic synthesis applications.

ACKNOWLEDGEMENTS

The authors NMP, AJ and MRP are greatly thankful to the Department of Chemistry, Jamshedpur Women's University, Jamshedpur and Nandurbar Taluka Vidhayak Samiti's G.T. Patil Arts, Commerce and Science College, Nandurbar, India for providing the necessary research facilities.

CONFLICT OF INTEREST

The authors declare that there is no conflict of interests regarding the publication of this article.

REFERENCES

1. S. Brahma, B. Nath, B. Basumatary, B. Das, P. Saikia, K. Patir and S. Basumatary, *Chemical Eng. J. Adv.*, **10**, 100284 (2022); https://doi.org/10.1016/j.ceja.2022.100284
2. M. Joyce Nirmala, P. Chandra Sekar, A. Johnson, U. Kizhuveetil, S. Shora and R. Nagarajan, *Fuel*, **351**, 128934 (2023); https://doi.org/10.1016/j.fuel.2023.128934
3. N. Ghosh, D. Rhithuparna, R. Khatoon, S.L. Rokhum and G. Halder, *J. Clean. Prod.*, **394**, 136362 (2023); https://doi.org/10.1016/j.jclepro.2023.136362
4. N.M. Marzouk, A.O.A. El Naga, S.A. Younis, S.A. Shaban, A.M. El Torgoman and F.Y. El Kady, *J. Environ. Chem. Eng.*, **9**, 105035 (2021); https://doi.org/10.1016/j.jece.2021.105035
5. K. Bonet-Ragel, A. Canet, M.D. Benaiges and F. Valero, *J. Chem. Technol. Biotechnol.*, **93**, 541 (2018); https://doi.org/10.1002/jctb.5399
6. A. Rodrigues, J.C. Bordado and R.G. Santos, *Energies*, **10**, 1817 (2017); https://doi.org/10.3390/en10111817
7. N. Akkarawatkhoosith, T. Tongtummachat, A. Kaewchada and A. Jaree, *Energy Convers. Manag.: X*, **11**, 100096 (2021); https://doi.org/10.1016/j.ecmx.2021.100096
8. E.S. Hanley, J.P. Deane and B.Ó. Gallachóir, *Renew. Sustain. Energy Rev.*, **82**, 3027 (2018); https://doi.org/10.1016/j.rser.2017.10.034
9. A. Azarafza, M.S. Ismail, M. Rezakazemi and M. Pourkashanian, *Renew. Sustain. Energy Rev.*, **116**, 109420 (2019); https://doi.org/10.1016/j.rser.2019.109420
10. M.O. Abdelmigeed, E.G. Al-Sakkari, M.S. Hefney, F.M. Ismail, T.S. Ahmed and I.M. Ismail, *Renew. Energy*, **174**, 253 (2021); https://doi.org/10.1016/j.renene.2021.04.057
11. R. Garg, R. Sabouni and M. Ahmadipour, *Ind. Crops Prod.*, **206**, 117554 (2023); https://doi.org/10.1016/j.indcrop.2023.117554
12. S. Ariaeenejad, E. Motamedi and G.H. Salekdeh, *Bioresour. Technol.*, **319**, 124228 (2021); https://doi.org/10.1016/j.biortech.2020.124228
13. P. Gu, S. Zhang, X. Li, X. Wang, T. Wen, R. Jehan, A. Alsaedi, T. Hayat and X. Wang, *Environ. Pollut.*, **240**, 493 (2018); https://doi.org/10.1016/j.envpol.2018.04.136
14. P. Wang, *Curr. Opin. Biotechnol.*, **17**, 574 (2006); https://doi.org/10.1016/j.copbio.2006.10.009
15. J. López-Fernández, M. Dolors Benaiges and F. Valero, *Bioresour. Technol.*, **334**, 125233 (2021); https://doi.org/10.1016/j.biortech.2021.125233
16. A. Cruz-Izquierdo, E.A. Pico, C. Lopez, J.L. Serra and M.J. Llama, *PLoS One*, **9**, e115202 (2014); https://doi.org/10.1371/journal.pone.0115202
17. M.R. Patil, S.D. Khairnar and V.S. Shrivastava, *Appl. Nanosci.*, **6**, 495 (2016); https://doi.org/10.1007/s13204-015-0465-z
18. M. Kordel, B. Hofmann, D. Schomburg and R.D. Schmid, *J. Bacteriol.*, **173**, 4836 (1991); https://doi.org/10.1128/jb.173.15.4836-4841.1991
19. M.A.A. Silva, R.A. Correa, M.G.O. Tavares and N.R.A. Filho, *Fuel*, **143**, 16 (2015); https://doi.org/10.1016/j.fuel.2014.10.048
20. I. Francolini, V. Taresco, A. Martinelli and A. Piozzi, *Enzyme Microb. Technol.*, **132**, 109439 (2020); https://doi.org/10.1016/j.enzmictec.2019.109439
21. M. Talebi, S. Vaezifar, F. Jafary, M. Fazilati and S. Motamedi, *Iran. J. Biotechnol.*, **14**, 33 (2016); https://doi.org/10.15171/ijb.1261
22. M.A. Alam, *Curr. Org. Chem.*, **23**, 978 (2019); https://doi.org/10.2174/1385272823666190424142821
23. A. Kumar, S. Mukhia, N. Kumar, V. Acharya, S. Kumar and R. Kumar, *Front. Bioeng. Biotechnol.*, **8**, 642 (2020); https://doi.org/10.3389/fbioe.2020.00642
24. M. Amirbandeh and A. Taheri-Kafrani, *Int. J. Biol. Macromol.*, **93**, 1183 (2016); https://doi.org/10.1016/j.ijbiomac.2016.09.092
25. Q. Xu, X. Bian, L. Li, X. Hu, M. Sun, D. Chen and Y. Wang, *Electrochem. Commun.*, **10**, 995 (2008); https://doi.org/10.1016/j.elecom.2007.12.002
26. Y. Ren, J.G. Rivera, L. He, H. Kulkarni, D.K. Lee and P.B. Messersmith, *BMC Biotechnol.*, **11**, 63 (2011); https://doi.org/10.1186/1472-6750-11-63
27. U.K. Jinwal, U. Roy, A.R. Chowdhury, A.P. Bhaduri and P.K. Roy, *Bioorg. Med. Chem.*, **11**, 1041 (2003); https://doi.org/10.1016/S0968-0896(02)00516-3
28. S. Kumar, K. Kikon, A. Upadhyay, S.S. Kanwar and R. Gupta, *Protein Express. Purif.*, **41**, 38 (2005); https://doi.org/10.1016/j.pep.2004.12.010
29. G.K. Joshi, S. Kumar, B.N. Tripathi and V. Sharma, *Curr. Microbiol.*, **52**, 354 (2006); https://doi.org/10.1007/s00284-005-0224-6
30. M.E. Hassan, Q. Yang and Z. Xiao, *Bull. Natl. Res. Cent.*, **43**, 102 (2019); https://doi.org/10.1186/s42269-019-0148-0
31. S.O. Kareem, O.Q. Adio and M.B. Osho, *Enzyme Res.*, **2014**, 1 (2014); https://doi.org/10.1155/2014/967056
32. K. Dumri and D.H. Anh, *Enzyme Res.*, **2014**, 389739 (2014); https://doi.org/10.1155/2014/389739
33. J.S. de Lima, M.P. Cabrera, C.M. de Souza Motta, A. Converti and L.B. Carvalho Jr, *Food Res. Int.*, **107**, 470 (2018); https://doi.org/10.1016/j.foodres.2018.02.066
34. J. Sulej, M. Osińska-Jaroszuk, M. Jaszek, M. Graz, J. Kutkowska, A. Pawlik, A. Chudzik and R. Bancerz, *Fungal Biol.*, **123**, 875 (2019); https://doi.org/10.1016/j.funbio.2019.09.007
35. S.A. Mohamed, M.H. Al-Harbi, Y.Q. Almulaiky, H. Ibrahim and R.M. El-Shishtawy, *Electron. J. Biotechnol.*, **27**, 84 (2017); https://doi.org/10.1016/j.ejbt.2017.03.010